Research Article

For reprint orders, please contact: reprints@futuremedicine.com

Nanomedicine

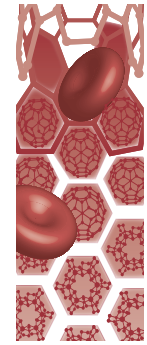

Light-triggered RNA release and induction of hMSC osteogenesis via photodegradable, dual-crosslinked hydrogels

Aim: To engineer a photodegradable hydrogel system for actively controlled release of bioactive unmodified RNA at designated time points to induce hMSC osteogenesis. **Materials & methods:** RNA/polyethylenimine complexes were loaded into dual-crosslinked photodegradable hydrogels to examine the capacity of UV light application to trigger their release. The ability of released RNA to drive hMSC osteogenic differentiation was also investigated. **Results & conclusion:** RNA release from photodegradable hydrogels was accelerated upon UV application, which was not observed in non-photodegradable hydrogels. Regardless of the presence of UV light, released siGFP exhibited high bioactivity by silencing GFP expression in HeLa cells. Importantly, siNoggin or miRNA-20a released from the hydrogels induced hMSC osteogenesis. This system provides a potentially valuable physician/patient-controlled 'on-demand' RNA delivery platform for biomedical applications.

First draft submitted: 4 March 2016; Accepted for publication: 4 May 2016; Published online: 1 June 2016

Keywords: bone tissue engineering • *in situ* forming hydrogel • miRNA • on-demand release • photolabile hydrogels • siRNA • stem cell differentiation • UV-controllable release

Cong Truc Huynh[‡,1], Minh Khanh Nguyen[‡,1], Mantas Naris[1], Gulen Yesilbag Tonga[2], Vincent M Rotello[2] & Eben Alsberg*[,1,3]

[1]Department of Biomedical Engineering, Case Western Reserve University, 10900 Euclid Avenue, Cleveland, OH 44106, USA

[2]Department of Chemistry, University of Massachusetts, 710 North Pleasant Street, Amherst, MA 01003, USA

[3]Department of Orthopaedic Surgery, Case Western Reserve University, 10900 Euclid Avenue, Cleveland, OH 44106, USA

*Author for correspondence:
Tel.: +1 216 368 6425
Fax: +1 216 368 4969
eben.alsberg@case.edu

[‡]Authors contributed equally

The global need for tissue and organ repair and replacement is exponentially increasing while the availability of donated organs for transplantation is far smaller than the demand [1–5]. Considerable recent scientific efforts have focused on identifying therapeutic alternatives to transplants. Tissue engineering using biocompatible biomaterials, cells, and/or inductive signals offers exciting potential strategies to regenerate lost and damaged tissue [1–5]. Mesenchymal stem cells (MSCs) are a particularly attractive cell source for tissue engineering and regenerative medicine applications because of their high capacity for culture expansion, low immunogenicity, and ability to differentiate into multiple connective tissue phenotypes [6–13]. MSCs can be isolated from many different tissue sources, such as bone marrow, placenta, umbilical cord blood, fat, muscle and corneal stroma [6,14–16]. When presented with specific signals in their microenvironment such as growth factors and genetic material, MSCs can be guided to differentiate down connective tissue cell lineages (e.g., chondrocytes, osteoblasts, myoblasts and adipocytes), which are valuable for engineering the corresponding tissues [4–6,16].

Delivering small interfering RNA (siRNA) or microRNA (miRNA) [17,18] to inhibit gene expression post-transcriptionally is a promising biomedical technology that has been investigated for many applications including cancer therapeutics [19–23], wound healing [24–26], and tissue regeneration [6–10,27–32]. For example, RNAs have been used in tissue regeneration to induce the differentiation of human MSCs (hMSCs) [6–10], canine MSCs [30] and rat MSCs [31] into osteoblasts [6–9,30,31], chondrocytes [10] or adipocytes [7,8]. siRNA suppresses gene activity by binding to one specific complementary

Future Medicine part of fsg

messenger RNA (mRNA) target and inactivating it through enzymatic cleavage [33–37], while miRNA regulates gene expression by binding to multiple mRNA targets and inhibiting their translation [17,18]. These RNAs possess great therapeutic potential due to their ability to regulate the production of specific proteins associated, for example, with the progression of a specific disease or the inhibition of tissue regeneration [6,20,32–38].

Despite the promise of siRNA and miRNA-based therapy, their effective delivery to target cells remains a significant challenge [1,6,32–48]. Efficacy of naked siRNA/miRNA is limited due to their short half-lives *in vivo*, ranging from several minutes to an hour, which is largely a consequence of their susceptibility to degradation by ribonucleases (RNases) [36]. Stability issues are further compounded by poor cellular uptake due to their high molecular weight, hydrophilicity, and negative charge [40]. To tackle these challenges, synthetic and natural materials have been examined to increase their delivery efficacy [34,49–52]. For example, nanocomplexes of anionic siRNA and miRNA with cationic macromers, such as polyethylenimines (PEIs) [46], chitosan [34,49], poly(β-amino ester) [21], and others [27,50,51] have been shown to increase their stability and cellular internalization. However, locally delivering these nanocarriers to specific regions in the body is hampered by their rapid dispersion *in vivo* as a result of their small size [6,32–38,47,52–54]. Consequently, repeated or high doses are generally necessary to achieve sustained gene knockdown at a target tissue.

Polymeric hydrogel biomaterials are three-dimentional chemically or physically crosslinked hydrophilic polymer networks that can absorb and retain large quantities of water [2,38,55–58]. Hydrogels hold great potential in biomedical and pharmaceutical applications because bioactive factors can be encapsulated within them and subsequently delivered in a localized and controlled manner at desired anatomic locations [38,55–57]. For example, they have been employed as depots for the delivery of anticancer drugs [59–61], genetic materials [62], and proteins [63–65]. Hydrogels have previously been engineered for localized, sustained and, in some cases, controlled delivery of siRNA/miRNA [1,6,39–42], where release was regulated via degradation in response to local environmental conditions surrounding the biomaterials and/or electrostatic interaction between RNA and the hydrogels [1,6,39–42]. However, once these RNA-containing biomaterials are injected or implanted into the body, neither the patient nor the clinician can alter the RNA release rate in response to potential temporal changes in the need for the therapeutic agent. To address this, we recently reported a photolabile hydrogel containing chemically-modified siRNA that can be uptaken by the cells without the need of a transfection reagent. This delivery occurs via electrostatic interaction between siRNA and hydrogel-incorporated primary amine groups and permits accelerated release of siRNA from the biomaterial via UV irradiation [47]. Although this system provides an innovative biomaterial platform for remote user-controlled 'on-demand' release of siRNA, retention of unmodified siRNA by the primary amines in the aforementioned hydrogels is challenging due to the necessity for unmodified siRNA complexation with a cationic transfection reagent for cellular internalization. Therefore, its potential applications may be restricted due to the limited availability of chemically-modified RNAs.

A hydrogel system capable of 'on-demand' controlled release of either unmodified or chemically-modified RNA using an external stimulus, such as UV, provides new directions in biomedical and tissue regeneration applications. This work reports a dual-crosslinked, photodegradable poly(ethylene glycol) (PEG) hydrogel system capable of accelerating the release of unmodified RNA post-gelation via UV application to induce hMSC osteogenic differentiation. The photodegradable PEG hydrogels were prepared using a combination of a Michael addition reaction between acrylate and thiol groups, and the oxidation of thiol groups. Hydrogel degradation and siRNA/PEI complex release profiles from the photodegradable hydrogels with and without UV stimulation were examined, and bioactivity of released siRNA against green fluorescent protein (siGFP) was investigated via the inhibition of GFP expression in destabilized GFP (deGFP)-expressing HeLa cells. Importantly, the ability of biological relevant RNA (e.g., siRNA against noggin or miRNA-20a) released from this photodegradable hydrogel system to induce osteogenic differentiation of hMSCs was demonstrated.

Materials & methods

Materials

Poly(ethylene glycol)-diacrylate (PEG-DA) and PEG-diphotodegradable-acrylate (PEG-DPA) macromers were synthesized as previously reported [47] and detailed in Supplementary Figure 1. 8-arm PEG-thiol ($PEG(-SH)_8$, Mw 10 kDa) was purchased from Jenkem Technology USA (TX, USA). Branched PEI (Mw 25 kDa), 1-methoxy phenazine methosulfate (PMS) and alizarin red S (ARS) were purchased from Sigma Aldrich (MO, USA). Hydrogen peroxide (H_2O_2) and sucrose were obtained from Fisher Scientific (PA, USA). 3-(4,5-dimethyl thiazol-2-yl)-5-(3-carboxy methoxyphenyl)-2-(4-sulfo phenyl)-2H-tetrazolium inner salt (MTS) was obtained from Promega Corporation (WI, USA).

siRNA targeting luciferase (siLuc, sequence 5′-GAU UAU GUC CGG UUA UGU AUU-3′) and siGFP (sequence 5′-GCA AGC UGA CCC UGA AGU UC-3′) are products of Dharmacon (CO, USA), and were obtained from Thermo Fisher Scientific (NY, USA). miRNA-20a (sequence 5′-UAA AGU GCU UAU AGU GCA GGU AG-3′), siNoggin (sequence 5′-AAC ACU UAC ACU CGG AAA UGA UGG G-3′) and nontargeting negative control siRNA (siCT, sequence 5′-UUC UCC GAA CGU GUC ACG UTT-3′) were purchased from Insight Genomics (VA, USA). Quant-iT™ RiboGreen® RNA reagent was obtained from Thermo Fisher Scientific.

High-glucose Dulbecco's Modified Eagle's Medium (DMEM-HG) and low-glucose DMEM (DMEM-LG) were purchased from Sigma. Phosphate-buffered saline (PBS), prescreened fetal bovine serum (FBS, Gibco), penicillin/streptomycin (P/S) and G-418 (50 mg/ml, Hyclone Laboratories Inc., UT, USA) were obtained from Fisher Scientific. hMSCs were isolated as reported in previous literature [6], stored under liquid nitrogen, plated at 5000 cells/cm^2, and cultured for 10 to 14 days before harvesting for use in experiments. deGFP-expressing HeLa cells were generously gifted from Dr. Matthew Levy (Albert Einstein College of Medicine, NY, USA).

Hydrogel preparation

The formation of the dual-crosslinked hydrogels is based on the combination of two synergistic chemistries including Michael addition (acrylate-thiol) and disulfide formation (Figure 1). The hydrogels were fabricated by simply mixing PEG-DPA or PEG-DA with PEG(-SH)$_8$ solutions at concentrations in PBS (pH 7.4) to achieve a thiol/acrylate molar ratio of 4/1 in 1.7 ml microcentrifuge tubes. The mixture (100 µl) was vortexed for 10 s, incubated at room temperature for 2 min to form the first crosslinks (acrylate-thiol), and then 1 µl PBS solution containing H_2O_2 (H_2O_2/SH = 1/1, mol/mol) was added and vortexed for 10 s to initiate the second crosslinking (disulfide bonds). The mixtures were incubated at room temperature for 2 h to achieve further gelation before conducting any experiments.

Hydrogel degradation

To determine the effect of UV light on the degradation of the dual-crosslinked photodegradable hydrogels, their degradation behavior in the absence or presence of UV light exposure was examined. The hydrogels were prepared as described in the previous section, rinsed in deionized water (diH_2O) and lyophilized, and their initial dried weights (W_{d0}) were measured. The dried hydrogels were rehydrated by immersion into PBS (10 ml, pH 7.4) and then incubated at 37°C. The PBS was changed every 3 days. Hydrogels were exposed to UV light (Omnicure S1000 UV, Lumen Dynamics Group, ON, Canada) at an intensity of 20 mW/cm^2 for 10 min ('UV 20–10') starting at day 0 and then weekly. At designated time points the hydrogels were collected, rinsed with diH_2O overnight at 4°C, frozen at -80°C and lyophilized, and their dried weights (W_{dt}) were then determined. The percentage mass loss was calculated by $(W_{d0}-W_{dt})/W_{d0}\times 100$.

Cytotoxicity of hydrogel degradation products

To determine cytotoxicity of hydrogel degradation products, the viability of HeLa cells and hMSCs when cultured with media containing various concentrations of degradation products was determined using an MTS assay. Hydrogels (4%, w/v) were prepared as described previously, immersed in 0.5 ml DMEM-HG and then divided into two groups. The first group was incubated at 37°C without UV light exposure to obtain hydrolytic degradation products upon complete degradation of the hydrogels by day 9. The second group was exposed to UV light at an intensity of 20 mW/cm^2 for 10 min ('UV 20–10'), 6 times/day until the hydrogels were completely degraded by day 4 to obtain photodegradation products.

Cells were seeded in monolayer in 48-well plates (Fisher Scientific) at a density of 25,000 and 20,000 cells/well for HeLa cells and hMSCs, respectively, in 250 µl of growth media and cultured at 37°C and 5% CO_2 in a humidified incubator. Growth media for HeLa cells and hMSCs consisted of DMEM-HG supplemented with 5% FBS and DMEM-LG supplemented with 10% FBS and 1% P/S, respectively. After 1 day of culture, the growth media was replaced with 250 µl growth media containing various concentrations of degraded hydrogels. The cells were cultured for an additional 2 days prior to executing the MTS assay.

To perform the MTS assay, sterile solutions of MTS (2 mg/ml) and PMS (0.92 mg/ml) were prepared in PBS (pH 7.4). Growth media in wells of 48-well plates containing HeLa cells or hMSCs was aspirated and the cells were rinsed with 0.5 ml PBS. Fresh PBS (200 µl) was added into each well followed by the addition of 50 µl freshly prepared MTS/PMS mixture (1/20, v/v). After 2 h incubation at 37°C and 5% CO_2 in a humidified incubator, 100 µl of solution in each well was transferred into wells of 96-well plates, and absorbance at 490 nm was recorded using a VERSAmax microplate reader (Molecular Devices Inc., CA, USA). The cells cultured with media only were used as a control ('Ctrl') with 100% cell viability, and the other samples were normalized to 'Ctrl' (n = 3).

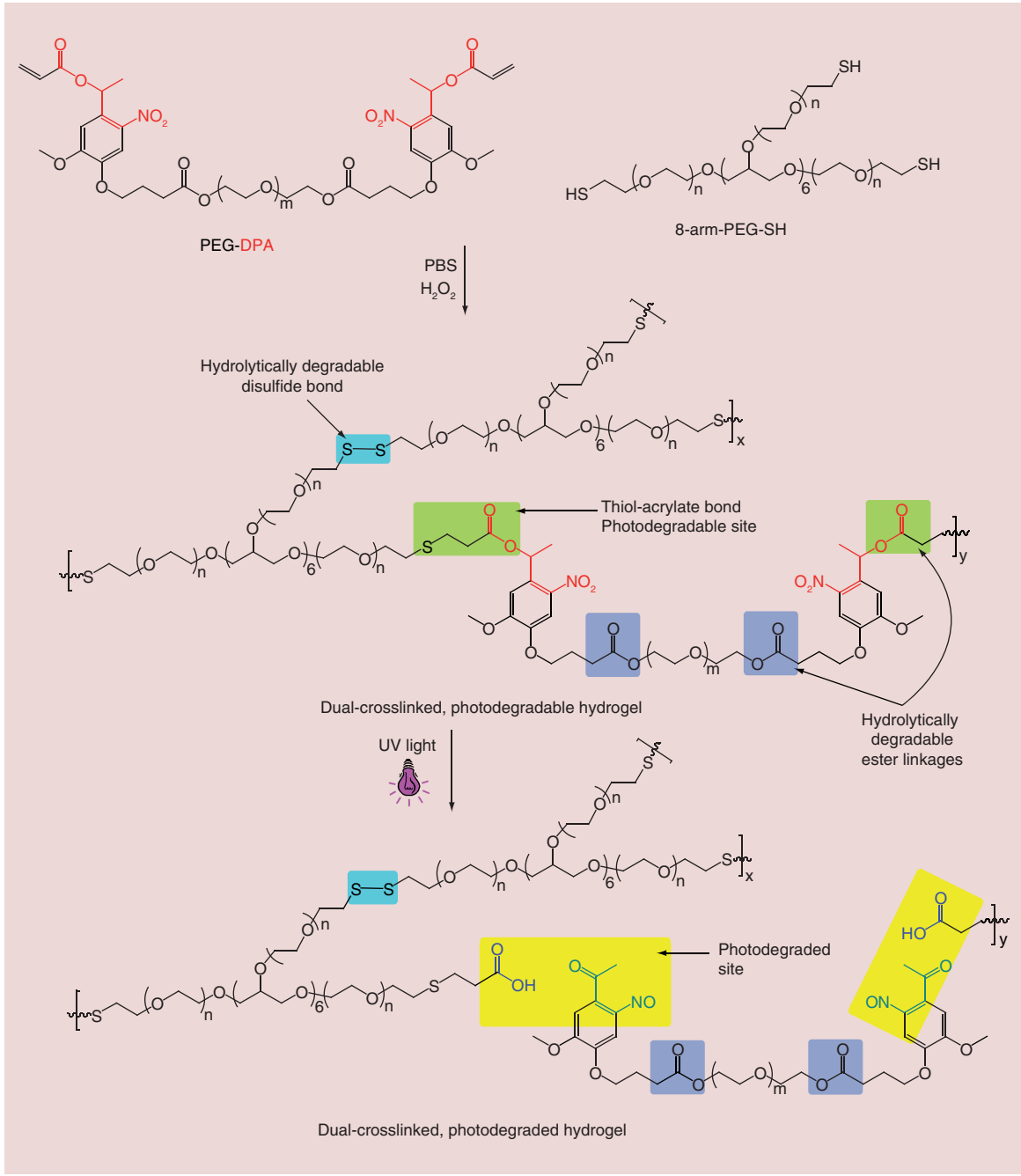

Figure 1. Schematic showing the formation of dual-crosslinked photodegradable hydrogels and their degradation when exposed to UV light.

siRNA loading & UV-triggered siRNA release in PBS

To examine the ability of UV light to accelerate the siRNA release rate from the hydrogels, the release kinetics of siRNA/PEI complexes were determined in PBS in the absence or presence of UV light exposure. Stock solutions of siRNA (100 μM) and PEI (1 mg/ml, 40 μM) in nuclease free water were separately prepared. siRNA/PEI complexes were formed using an N/P ratio of 11.5, where N and P are the number of amine and phosphate groups in PEI and siRNA, respectively, by adding diluted siRNA solution (12.8 μM) to the same volume of diluted PEI solution (9.6 μM) in PBS, vortexing the mixture for 30 s and then incubating it at room temperature for 30 min. The prepared siRNA/PEI complexes were then loaded into PEG-DPA or PEG-DA solutions in 1.7 ml nuclease free tubes (Fisher Scientific) and $PEG(\text{-}SH)_8$ solu-

tions were added to prepare the hydrogels (100 µl, 4 µg siRNA/gel) as described previously. Then, 1 ml PBS (pH 7.4) was added into each tube and the release was carried out at 37°C. At predetermined time points, the released media was collected and 1 ml fresh PBS was added. UV light was applied to hydrogels in the exposure treated groups at day 0 and either at every collection time point or weekly prior to the addition of fresh PBS. A standard curve was established by diluting a freshly prepared siRNA/PEI complex solution (6.4 µM or 80 µg/ml) in fresh media into a series of known concentrations (0 to 4 µg/ml). The releasates and standard samples (10 µl) were mixed with a heparin solution (Sigma, 5 µl solution 10 mg/ml) for 30 min to disassociate siRNA/PEI complexes and free siRNA was quantified using a RiboGreen RNA assay with fluorescence values measured using a plate reader (fmax, Molecular Devices Inc.) set at excitation 485/emission 538 nm [6,47].

Release behavior of siRNA/miRNA in DMEM

To examine the bioactivity of released siRNA/miRNA, lyophilized RNA/PEI complexes were encapsulated in photodegradable hydrogels, their release kinetics in phenol red-free DMEM with and without application of UV light were measured, and the released siRNA/miRNA was then used to transfect cells cultured in monolayer. Lyophilized RNA/PEI complexes prepared in the presence of lyo-protectants such as sucrose [1] or trehalose [27] have been reported to help retain the bioactivity of RNA materials. Retention of siRNA bioactivity using this strategy was confirmed in this report (Supplementary Figure 2). To prepare the lyophilized RNA/PEI complexes, diluted siRNA/miRNA (4.0 µM) and PEI (3.0 µM) solutions in PBS supplemented with 10% sucrose were mixed, vortexed for 60 s and incubated at room temperature for 30 min, followed by freezing at -80°C for 2–4 h and lyophilizing for at least 16 h. The lyophilized RNA/PEI complexes were then mixed with PEG-DPA solution and the siRNA/miRNA-loaded hydrogels (50 µl, 5 µg RNA/gel) were fabricated as described previously. Prior to release studies, the hydrogels were rinsed with 0.5 ml phenol red-free DMEM at 4°C for 3 h to remove sucrose, and the amount of RNA in the rinse solutions was measured using the RiboGreen assay and subtracted from the total amount initially loaded to obtain the true loaded-amount for the subsequent release experiments. Less than 5% of the total amount originally loaded was measured in the rinse solutions. The release of siRNA/miRNA was carried out in phenol red-free DMEM (DMEM-HG for siGFP and DMEM-LG for siNoggin/miRNA-20a) in the absence or presence of UV light as described above. Designated hydrogels were directly exposed to UV at an intensity of 2 mW/cm^2 for 10 min ('UV 2–10') every day while they persisted. The concentration of siRNA/miRNA in releasates was quantified as described earlier.

Bioactivity of released siGFP on deGFP-expressing HeLa cells in monolayer

deGFP-expressing HeLa cells were seeded in monolayer in wells of 24-well plates (Fisher Scientific) at a density of 50,000 cells/well in 0.5 ml of DMEM-HG supplemented with 5% FBS and G-418 (250 µg/ml), and cultured at 37°C and 5% CO_2 in a humidified incubator. After 1 day of culture, the growth media in each well was replaced with 0.5 ml of pooled releasates from 3 hydrogels at a given time point of 'No UV' or daily 'UV 2–10'-treated (starting at day 0 or day 6) groups (22.5% (w/v) photodegradable hydrogels) [47]. The cells were cultured for 6 h, and then the media was replaced with 0.5 ml of fresh culture media without G-418. The cells were cultured for an additional 2 days before harvesting for flow cytometry (EPICS XL-MCL, Beckman Coulter, CA, USA) to quantify the degree of GFP silencing. Lyophilized siRNA/PEI complexes were freshly reconstituted in DMEM-HG and used as a knockdown positive control ('Pos. Ctrl'). Cells transfected with media only served as a nontransfected control ('Ctrl') and were considered to exhibit 100% GFP expression, and all other groups were normalized to the 'Ctrl'.

Osteoinductivity of UV-triggered released siNoggin/miRNA-20a on hMSCs in monolayer

hMSCs were seeded in wells of 24-well plates at a density of 10,000 cells/well in 0.5 ml of DMEM-LG supplemented with 10% FBS and 1% P/S. After 1 day of culture, growth media in each well was replaced with 0.5 ml of DMEM-LG containing released siNoggin or miRNA-20 (40 nM). After culturing for 6 h, the transfection media in each well was replaced with 0.5 ml osteogenic media (i.e., DMEM-LG supplemented with 10% FBS, 1% P/S, 100 nM dexamethasone [MP Biomedicals, OH, USA], 10 mM b-glycerophosphate [CalBiochem, MA, USA] and 100 µM ascorbic acid [Wako USA, VA, USA]). The osteogenic media was replaced twice per week. After 3 weeks, the media was removed, and cells were rinsed with 0.5 ml PBS. The cells were then fixed with a 70% solution of ice-cold ethanol in diH_2O (v/v) at 4°C for 1 h, after which they were rinsed with 0.5 ml diH_2O. The cells were stained with ARS solution (60 mM, pH 4.1) for 10 min and then rinsed twice with 0.5 ml of diH_2O and once with 0.5 ml of PBS (pH 7.4) for 15 min before being imaged using a TMS-F microscope (Nikon, Japan) with a mounted Nikon E995 camera (Nikon,

Japan). Calcium-bound dye in each well was dissolved with 0.5 ml of 10% (w/w) cetylpyridinium chloride (CPC, Sigma) in 10 mM sodium phosphate buffer at pH 7.0 for 30 min at room temperature, after which 100 µl of solution was transferred to wells of 96-well plates for ARS quantification by recording absorbance at 562 nm [66] using a VERSAmax microplate reader (Molecular Devices Inc.). Cells transfected with DMEM-LG only, freshly reconstituted lyophilized siNoggin and siCT were used as a nontransfected control group ('Ctrl'), a knockdown positive control ('Pos. Ctrl') and a negative control ('Neg. Ctrl'), respectively. The concentrations of ARS in PBS solution (pH 7.0) containing CPC (10% w/v) were reported to be linearly related to the absorbance of the ARS solutions [67,68] and bound calcium amounts [66]; and therefore the absorbance ratios between groups are considered to be their deposited calcium ratios.

Statistical analysis

The data are expressed as mean ± standard deviation (n = 3). Statistical analysis was performed with one-way analysis of variance (ANOVA) with Tukey–Kramer Multiple Comparisons using GraphPad Instat 3.0 software (GraphPad Software Inc., CA, USA). $p < 0.05$ was considered to be statistically significant.

Results & discussion

Hydrogel formation & photodegradation

The dual-crosslinked hydrogels were prepared using a combination of two crosslinking chemistries: acrylate and thiol addition reaction and disulfide formation. PEG-DA and PEG-DPA were used as acrylate macromers for preparing non-photodegradable and photodegradable hydrogels, respectively. The hydrogels were prepared by mixing PEG-DA or PEG-DPA with excess $PEG(\text{-}SH)_8$ to allow the formation of the acrylate-thiol crosslinks for 2 min, followed by the addition of H_2O_2 to initiate the formation of disulfide bonds as the second crosslink. Gelation occurred 3–5 min after mixing the acrylate and thiol solutions depending on the macromer concentrations. Figure 1 shows a schematic of dual-crosslinked photodegradable hydrogel formation and hydrogel photodegradation upon the application of UV light.

Bioactive factors and cells can easily be encapsulated within hydrogels for tissue engineering applications [2,5,6,38,55–58]. The degradation of hydrogel biomaterial platforms increases their network pore size, which regulates the release of loaded bioactive molecules, creates free space for newly forming tissues and enhances transport of oxygen and nutrients to encapsulated cells as well as removal of metabolic waste. In this photocleavable hydrogel system, the degradation rate was actively controlled post gelation by applying UV light to degrade photodegradable linkages within the hydrogel networks. Degradation profiles of 22.5% (w/v) hydrogels with and without the weekly application of UV light at an intensity of 20 mW/cm^2 for 10 min ('UV 20–10') were measured. Without UV application ('No UV'), hydrogels gradually decreased their mass, with 46% mass loss after 4 weeks (Figure 2A) due to hydrolytic degradation of ester groups in the network [6,41,47]. However, when subjected to external UV light, the degradation rate of 'UV 20–10' hydrogels was accelerated, as expected, with 83% mass loss after 4 weeks (Figure 2A). This increase in the degradation rate of the 'UV 20–10' hydrogels was attributed to the photodegradation of photocleavable linkages in the biomaterial network [47,69,70]. Photographs of 6 mm hydrogel discs (22.5%, w/v) exposed to UV light at an intensity of 20 mW/cm^2 for different periods of time (0 to 60 min, Figure 2B) depict a change in appearance from transparent to dark yellow due to the photodegradation of photolabile linkages.

Cytotoxicity of degradation products

Hydrogel degradation products contain carboxylic acid and hydroxyl groups from hydrolytic degradation and/or acetal derivative and free carboxylic acid groups from photodegradation [69]. To examine potential cytotoxicity, monolayer cells were exposed to different concentrations of the degradation products in culture media and their viability was then measured indirectly after 2 days using an MTS assay. Viability of HeLa cells and hMSCs was minimally affected at degradation product concentrations of 0.38 mg/ml or less (Figure 3). Viability of both cell types decreased as degradation product concentration increased above 0.38 mg/ml, with less than 79.7% average viability at 3.00 mg/ml (Figure 3). There was no significant difference in cell viability between the cells treated with hydrolytically degraded gels and photolytically degraded gels.

UV-controllable siRNA release

After demonstrating that the engineered photolabile hydrogels degraded in response to UV light, the ability to trigger siRNA release from the hydrogels by exposing them to UV was investigated. To examine this release capability of the biomaterial system, siRNA/PEI complexes (using siLuc) were physically encapsulated in the hydrogels, and the siRNA-loaded hydrogels were exposed to UV light to determine if release of the loaded genetic material could be controlled. Figure 4 shows a schematic of UV-triggered degradation of the hydrogels and the subsequent release of siRNA/PEI complexes from the network in aqueous media.

The release of siRNA from non-photodegradable hydrogels was first performed in both the absence and presence of UV light to confirm UV-independence of the siRNA release kinetics. As expected, siRNA was released from 'No UV' and 'UV-1' non-photodegradable hydrogels at the same rate, with approximately 30 and 63% cumulative siRNA released after 4 and 10 days, respectively, indicating a UV-independent release mechanism (Figure 5A). To demonstrate the ability of UV to regulate siRNA release from the photodegradable hydrogels, the release of siRNA from 15% (w/v) hydrogels was performed. siRNA was gradually released from the 'No UV' hydrogels, with 55% cumulative siRNA released after 3 weeks (Figure 5B), likely governed by the hydrolytic degradation of ester groups (hydrolytic degradable sites in Figure 1) in the hydrogel networks [6,41,47]. In contrast, siRNA release from 'UV-2' 15% (w/v) hydrogels was significantly accelerated beginning at day 3, and 94% of siRNA was cumulatively released after 3 weeks (Figure 5B). This acceleration in siRNA release rate was a result of UV light exposure mediated photodegradation of the hydrogel networks [47], which was confirmed by the degradation results (Figure 2A). The persistence time of the 15% (w/v) photodegradable hydrogels was more than 9 weeks (Supplementary Figure 3A), regardless of the absence or presence of UV exposure, likely due to the slow and UV-independent degradation of disulfide bonds in the networks.

To demonstrate the ability to tune siRNA release from the hydrogel system, siRNA release from 22.5% (w/v) hydrogels was next examined with various UV doses. By increasing the hydrogel concentration from 15 to 22.5% (w/v), the siRNA release rate substantially decreased in 'No UV' hydrogels. After 4 weeks, 27% siRNA released from the 'No UV' 22.5% (w/v) hydrogels (Figure 5C) compared to 59% from the 'No UV' 15% (w/v) hydrogels (Figure 5B). These findings are in agreement with the literature as increasing hydrogel concentration and/or crosslinking density have been reported to decrease the release rate of loaded bioactive molecules such as siRNA, anticancer drugs and proteins from the hydrogel networks [47,57,60,63,71]. Similar to the 15% (w/v) hydrogels, siRNA release was accelerated when the 22.5% (w/v) hydrogels were exposed to external UV light

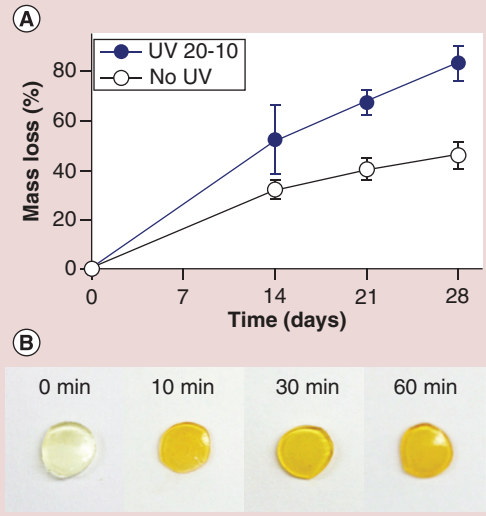

Figure 2. (A) Degradation profiles of 22.5% (w/v) dual-crosslinked photodegradable hydrogels in the absence or presence of UV light at an intensity of 20 mW/cm^2 for 10 min ('UV 20–10') weekly. **(B)** Photographs of 6 mm hydrogel discs (22.5%, w/v) exposed to UV light at an intensity of 20 mW/cm^2 for different periods of time.

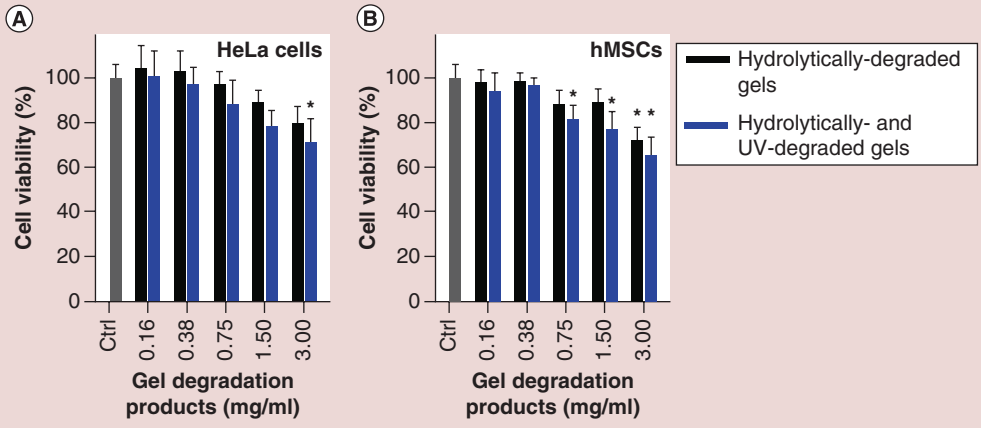

Figure 3. Viability of (A) HeLa cells and (B) hMSCs measured indirectly using an MTS assay after 2 days with degradation products of photodegradable dual-crosslinked hydrogels in the culture media.
*$p < 0.05$ compared with corresponding 'Ctrl' group.

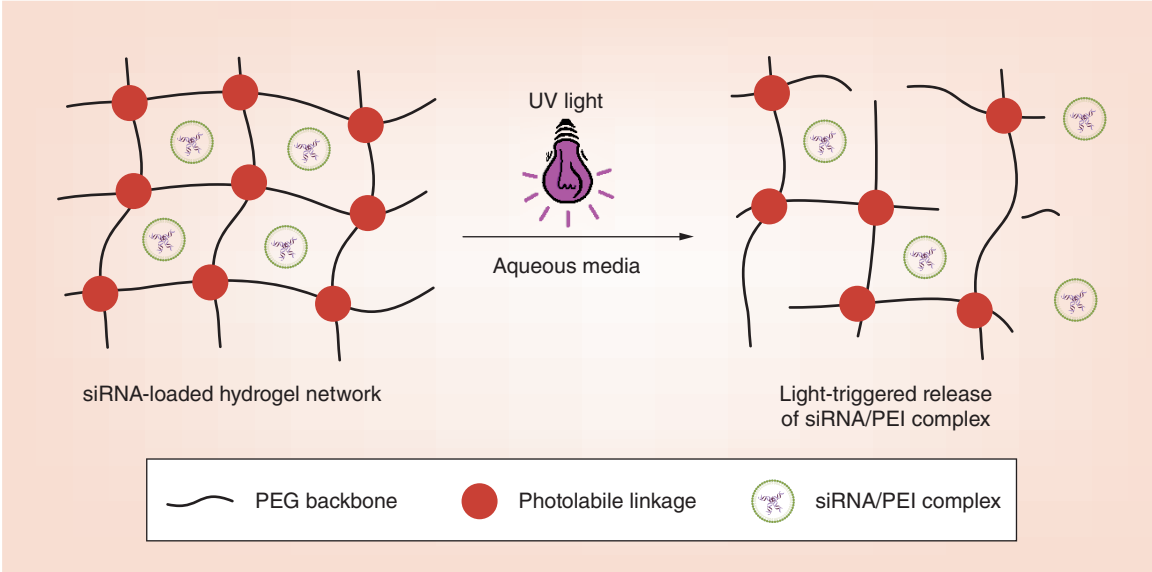

Figure 4. Schematic showing UV-triggered degradation of hydrogels and the subsequent release of siRNA/PEI complexes.

(Figure 5C, 'UV-3': 20 mW/cm^2 for 10 min at each release time point or 'UV-4': 20 mW/cm^2 for 30 min weekly). siRNA was released from the 'UV-3' and 'UV-4' hydrogels at the same rate for the first 2 weeks, likely due to the same cumulative duration of UV exposure (i.e., a total of 60 min) at an intensity of 20 mW/cm^2. After 2 weeks, however, the siRNA release rate from the 'UV-4' hydrogels was higher than that from the 'UV-3' hydrogels as a result of increased cumulative UV exposure time (Figure 5C, UV-4/UV-3 (min exposure/min exposure): 60/60 at day 10, 90/70 at day 14, 120/80 at day 21, 150/90 at day 28). The hydrogels in Figure 5C were completely degraded by 9 weeks (Supplementary Figure 3B) regardless of the UV light application, likely due to the contribution of the slowly degrading disulfide bonds in the network. Overall, this dual-crosslinked photodegradable hydrogel system can be used for sustained release of siRNA with a capacity to actively elevate the release rate at designated time points by directly applying an external UV light source to the hydrogels.

Although macroscopic hydrogel and scaffold biomaterials have recently been reported to provide localized, sustained, and in some cases controlled release RNA, release could not be controlled after gelation. The RNA release rates were adjusted by tailoring the degradation rate of the hydrogel networks [1,6,21,27,39–41] and the affinity between RNA molecules and functional groups incorporated in the hydrogels [39–42]. In contrast, the approach reported here provides a flexible strategy to accelerate siRNA release from photolabile hydrogel networks 'on-demand' at designated time points via exposure to a UV light source.

Silencing GFP expression in deGFP-expressing HeLa cells with released siGFP

Having demonstrated the ability of the hydrogel system to tune and accelerate siRNA release via UV application in PBS, released siRNA bioactivity was then assessed. siGFP released from the hydrogels in phenol red-free DMEM-HG was examined in the absence or presence of daily UV light exposure at an intensity of 2 mW/cm^2 for 10 min ('UV 2–10'). siGFP release concentration was first measured, and siGFP was gradually released from 'No UV' hydrogels in a sustained fashion over a release course lasting 5 weeks (Figure 6). As predicted, UV irradiation triggered siGFP release in DMEM-HG by facilitating the degradation of photodegradable linkages in the hydrogel network, which resulted in an increased siRNA release rate ('UV' hydrogels, Figure 6) and shorter hydrogel persistence times. Hydrogels in all groups were completely degraded by their last release time point, which occurred at day 18, 20 and 35 for 'UV,' 'UV from D6' and 'No UV' hydrogels, respectively (Figure 6). Interestingly, the release rate of siGFP was rapidly accelerated when the hydrogels were exposed to UV starting at day 6 in the 'UV from D6' group, indicating that external UV light stimulation can actively trigger the release rate of siGFP at a designated time point. In addition, the retention time of the hydrogels in DMEM-HG was much shorter than that in PBS (i.e., 35 days in DMEM-HG compared with 63 days in PBS for 22.5% (w/v) 'No UV' hydrogels, Figure 6 & Supplementary Figure 3B), but it is not clear why the differences in the solution compositions dramatically influenced the degradation rates of the hydrogels.

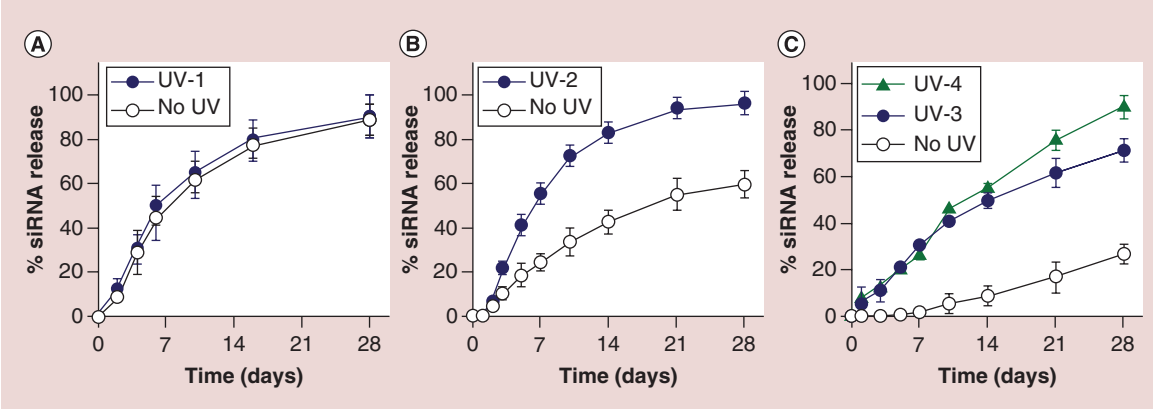

Figure 5. Release profiles of siRNA from (A) 15% (w/v) non-photodegradable and (B) 15% (w/v) and (C) 22.5% (w/v) photodegradable dual-crosslinked hydrogels in PBS in the absence or presence of UV light exposure.
'UV-1': 5 mW/cm^2 for 10 min at each time point; 'UV-2': 10 mW/cm^2 for 10 min at each time point; 'UV-3': 20 mW/cm^2 for 10 min at each time point; 'UV-4': 20 mW/cm^2 for 30 min weekly.

To assess the bioactivity of siRNA released from the hydrogels in DMEM-HG, deGFP-expressing HeLa cells in 24 well plates were treated with the pooled releasates at specific time points, and the degree of GFP silencing was examined using flow cytometry. The releasates from the different hydrogel groups at specific time points containing different amounts of released siGFP (Figure 7A) silenced GFP expression to different degrees. GFP expression of deGFP-expressing HeLa cells was measured at day 2 following transfection with the released siGFP (Figure 7B). Cells cultured with media only were assigned as a nontransfected 'Ctrl' group that was considered to exhibit 100% GFP expression. Cells transfected with day 14 (D14) releasates from hydrogels that did not contain siGFP but were exposed to UV, a negative control ('Neg. Ctrl'), expressed 100% GFP, indicating that the degraded hydrogels themselves did not cause GFP silencing (Figure 7B). Importantly, cells cultured with releasates from both 'UV' and 'No UV' siGFP-loaded hydrogels significantly reduced GFP expression in comparison to the 'Ctrl,' indicating that the released siGFP retained its bioactivity. Cells cultured with freshly reconstituted lyophilized siGFP/PEI complexes, a knockdown positive control ('Pos. Ctrl'), exhibited a high degree of gene silencing with 18% GFP expression due to the relatively high siRNA concentration (80 nM) applied (Figure 7A). GFP expression of the cells transfected with day 2 (D2) releasates from all groups was not significantly different from (i.e., 'No UV' and 'UV from D6') or significantly lower than (i.e., 'UV') that of the 'Pos. Ctrl' groups (Figure 7B), due to similar or higher released siGFP concentrations in the transfection media (Figure 7A), indicating the high bioactivity of released siGFP. At each specific time point, the releasates with higher siGFP concentration resulted in increased GFP silencing. For example, the same siGFP concentration in day 6 (D6) releasates from the 'No UV' and 'UV from D6' hydrogels (Figure 7A) exhibited the same degree of GFP silencing (Figure 7B). However, D6 releasates from the 'UV' hydrogels decreased GFP silencing more compared with that from the 'No UV' and 'UV from D6' hydrogels (Figure 7B), due to the higher concentration of released siGFP (Figure 7A). Interestingly, when UV was turned on at day 6, the siGFP concentration of day 8 (D8) releasates from the 'UV from D6' hydrogels abruptly increased, leading to decreased GFP expression compared with the 'No UV' and 'UV' hydrogels (Figure 7). This result also demonstrated that UV stimulation could accelerate the release rate of siRNA from the hydrogels and subsequently suppressed gene expression of cells at a specific time point in an 'on-demand' manner. This actively controlled release of genetic material could be valuable for biomedical applications such as cancer treatment and tissue engineering.

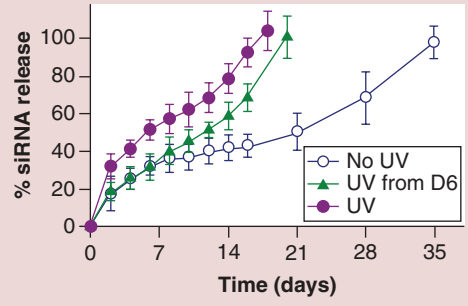

Figure 6. Release of siGFP from 22.5% (w/v) photodegradable dual-crosslinked hydrogels in the absence or presence of daily UV light exposure at an intensity of 2 mW/cm^2 for 10 min ('UV 2–10', starting at day 0 or day 6) in phenol red-free DMEM-HG.

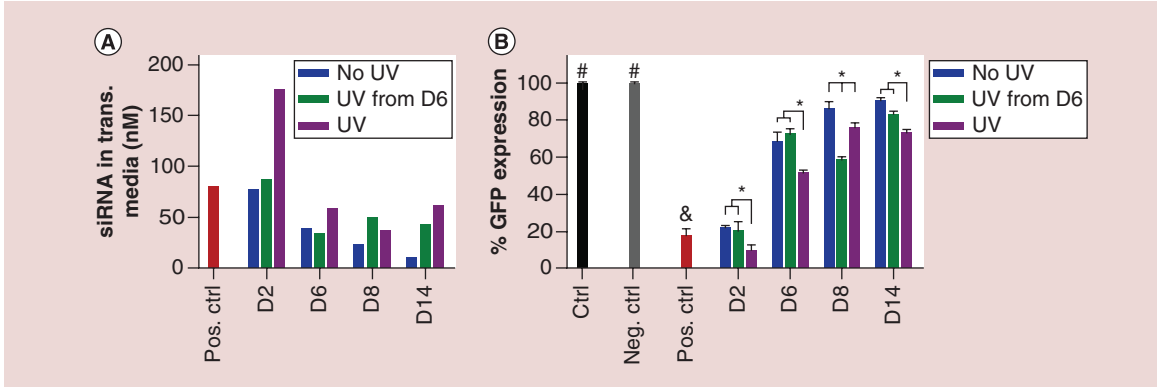

Figure 7. (A) Concentration of released siGFP used in the transfection media for the bioactivity study and **(B)** GFP expression of deGFP-expressing HeLa cells cultured in monolayer and transfected with all releasates that were collected at predetermined time points from dual-crosslinked photodegradable hydrogels in the absence or presence of daily UV light exposure at an intensity of 2 mW/cm2 for 10 min ('UV 2–10,' starting at day 0 or day 6). 'Neg. Ctrl': cells transfected with day 14 releasates from no-siGFP 'UV' hydrogels; 'Pos. Ctrl': cells transfected with freshly reconstituted lyophilized siGFP/PEI complexes (80 nM).
#$p < 0.05$ compared with groups that do not contain the same symbol, and $p < 0.01$ compared with 'UV' group at D2 and all groups at D6, D8 and D14.
*$p < 0.05$.

UV light-triggered release of RNA to drive osteogenic differentiation of hMSCs cultured in monolayer

This photodegradable hydrogel system has been engineered to trigger siRNA release via the application of an external UV light source, and regardless of the presence of UV light, the released siGFP retains its bioactivity as evidenced by its capacity to silence GFP expression in HeLa cells. To further examine the potential application of this hydrogel system in tissue engineering and regenerative medicine, the capacity of UV-light-triggered release of biologically relevant RNAs, specifically siNoggin and miRNA-20a, to induce osteogenic differentiation of hMSCs cultured in monolayer was investigated. siNoggin has been reported to enhance osteogenic differentiation of hMSCs by downregulating the expression of noggin protein, which is a bone morphogenetic protein (BMP) antagonist that inhibits BMPs from binding to their receptors on the cell surface [6,72–75]. miRNA-20a can also guide hMSC osteogenic differentiation by downregulating Bambi, Crim1 and peroxisome-proliferator-activated receptor (PPARγ), which are antagonists of BMP pathway [9,76].

Using this hydrogel system, UV light could be used to tailor the release profile of encapsulated siNoggin. In the absence of UV light, siNoggin was slowly released in a sustained fashion from 'No UV' hydrogels over the course of 5 weeks (Figure 8A). In contrast, siNoggin was released from 'UV' hydrogels at a faster rate, and all loaded siNoggin was recovered by day 19 when the hydrogels were completely degraded. To assess the ability of the released siNoggin (40 nM) to direct hMSC osteogenic differentiation, releasates at certain time points were used to transfect hMSCs cultured in monolayer, and the cells were cultured in osteogenic media for up to 3 weeks. After 3 weeks of culture, calcium deposition, a primary indicator of hMSC osteogenic differentiation, was stained with ARS and then quantified. A low density of deposited calcium was observed in the 'Ctrl' group, which was cultured in DMEM-LG without siRNA (Figure 8B). Similarly, cells transfected with day 4 (D4) releasates from empty 'UV'-treated hydrogels (without siRNA, 'Gel only') and lyophilized siCT/PEI complexes ('siCT' at 40 nM) showed a low density of deposited calcium (Figure 8B). Calcium quantification confirmed that amounts of deposited calcium normalized to the 'Ctrl' group were similar in the 'Gel only', 'siCT' and 'Ctrl' groups (Figure 8C). As expected, the freshly reconstituted lyophilized siNoggin ('Pos. Ctrl' at 40 nM) and siNoggin released from the 'No UV' and 'UV' hydrogels at the day 2 (D2) and day 4 (D4) time points increased deposited calcium density in ARS red staining images (Figure 8B) and quantified calcium deposition (Figure 8C). BMP-2 expression increases when the hMSCs differentiate into osteoblasts [74], and the expression of noggin, an antagonist of BMP, is then upregulated [75]. Therefore, presentation of siNoggin, as released in this system, suppresses the expression of noggin, enhances BMP signaling and promotes osteogenesis of hMSCs [6,72–75]. These results indicate that, regardless of the absence or presence of 'UV 2–10', the released siNoggin from the hydrogels retained its bioactivity and induced the osteogenic differentiation of hMSCs.

Although the released siNoggin retained its bioactivity as demonstrated by an enhancement in the osteogenic differentiation of hMSCs compared with the 'Gel

only,' 'siCT' and 'Ctrl' groups, a decrease in the relative amount of deposited calcium was observed in groups treated with the released siNoggin from the both 'UV' and 'No UV' hydrogels. Specifically, while the 'Pos. Ctrl' group produced 3.5-fold higher calcium deposition than the 'Ctrl' group, siNoggin released from the 'UV' hydrogels at D2 and D4 or from the 'No UV' hydrogels at D4 exhibited only 2.1–2.6-fold higher calcium deposition than the 'Ctrl' group. This decrease in the degree of osteogenic induction of the released siNoggin may have been due to binding of hydrogel degradation products containing carboxylic acid groups to the positively charged siNoggin/PEI nanocomplexes [77,78]. This binding might cause a decrease in the surface charge density of nanocomplexes and increase the particle size, and subsequently decrease their ability to be internalized by cells [79]. Importantly, at both D2 and D4 time points, the released siNoggin from the both 'No UV' and 'UV' hydrogels showed a similar amount of deposited calcium (Figure 8C), indicating that the UV application had little effect on the bioactivity of released siNoggin.

Similar to siNoggin, miRNA-20a release from the photodegradable hydrogels was also triggered by UV

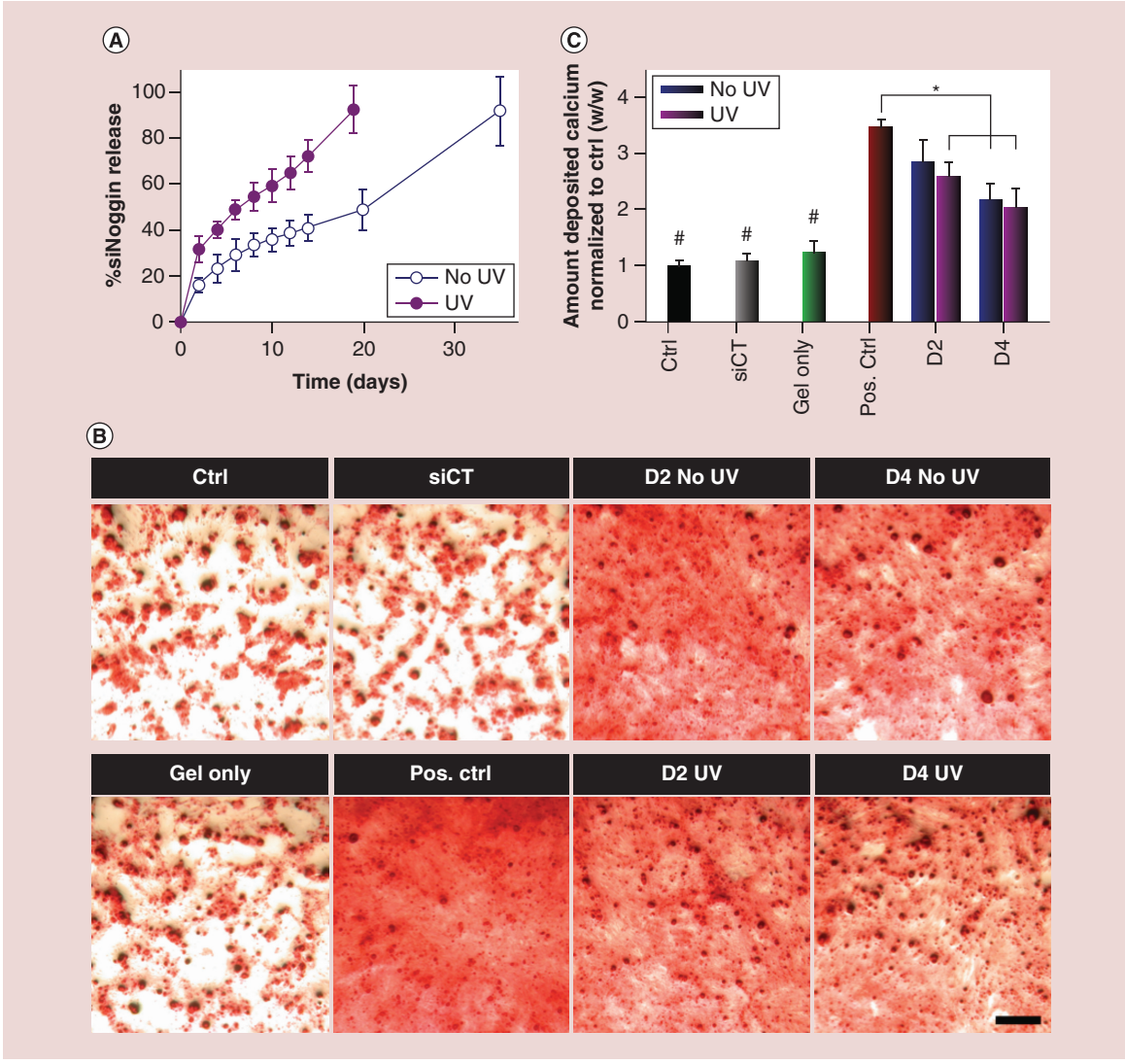

Figure 8. **(A)** siNoggin release behavior from 22.5% (w/v) photodegradable hydrogels into DMEM-LG in the absence or presence of 'UV 2–10' daily. **(B)** Photomicrographs of ARS staining depicting the deposition of calcium, and **(C)** quantification of deposited calcium (normalized to 'Ctrl') by hMSCs cultured in monolayer and transfected with the same concentration (40 nM) of released siNoggin from hydrogels at day 2 (D2) or day 4 (D4) or freshly reconstituted lyophilized siRNA/PEI complexes of siCT ('siCT') or siNoggin ('Pos. Ctrl'). 'Gel only': pooled D4 releasates from 'UV'-treated hydrogels lacking RNA. The scale bar indicates 200 μm.
#$p < 0.05$ compared with groups that do not contain the same symbol.
*$p < 0.05$.

stimulation (Figure 9A). Specifically, miRNA-20a was released from the 'No UV' and 'UV' hydrogels over the course of 37 and 20 days, respectively. The same amounts of released miRNA-20a (40 nM) were then used to transfect hMSCs to examine its ability to induce osteogenic differentiation [9]. The released miRNA-20a from both 'No UV' and 'UV' hydrogels increased the osteogenic differentiation of hMSCs compared with the 'Gel only', 'siCT' and 'Ctrl' groups, as evidenced by the increased calcium deposition in ARS staining photomicrographs (Figure 9B) and quantified deposited calcium (Figure 9C). Regardless of UV light exposure, the released miRNA-20a at D2 showed a similar amount of deposited calcium to the 'Pos. Ctrl' group at a concentration of 40 nM, which exhibited a 3.3-fold increase compared with the 'Ctrl' group (Figure 9C). Although the amount of deposited calcium by cells treated with the released miRNA-20a from D4 was lower than that of the 'Pos. Ctrl,' the amounts of deposited calcium in groups treated with the released miRNA-20a from the 'No UV' and 'UV' hydrogels are similar at all experimental time points (Figure 9C).

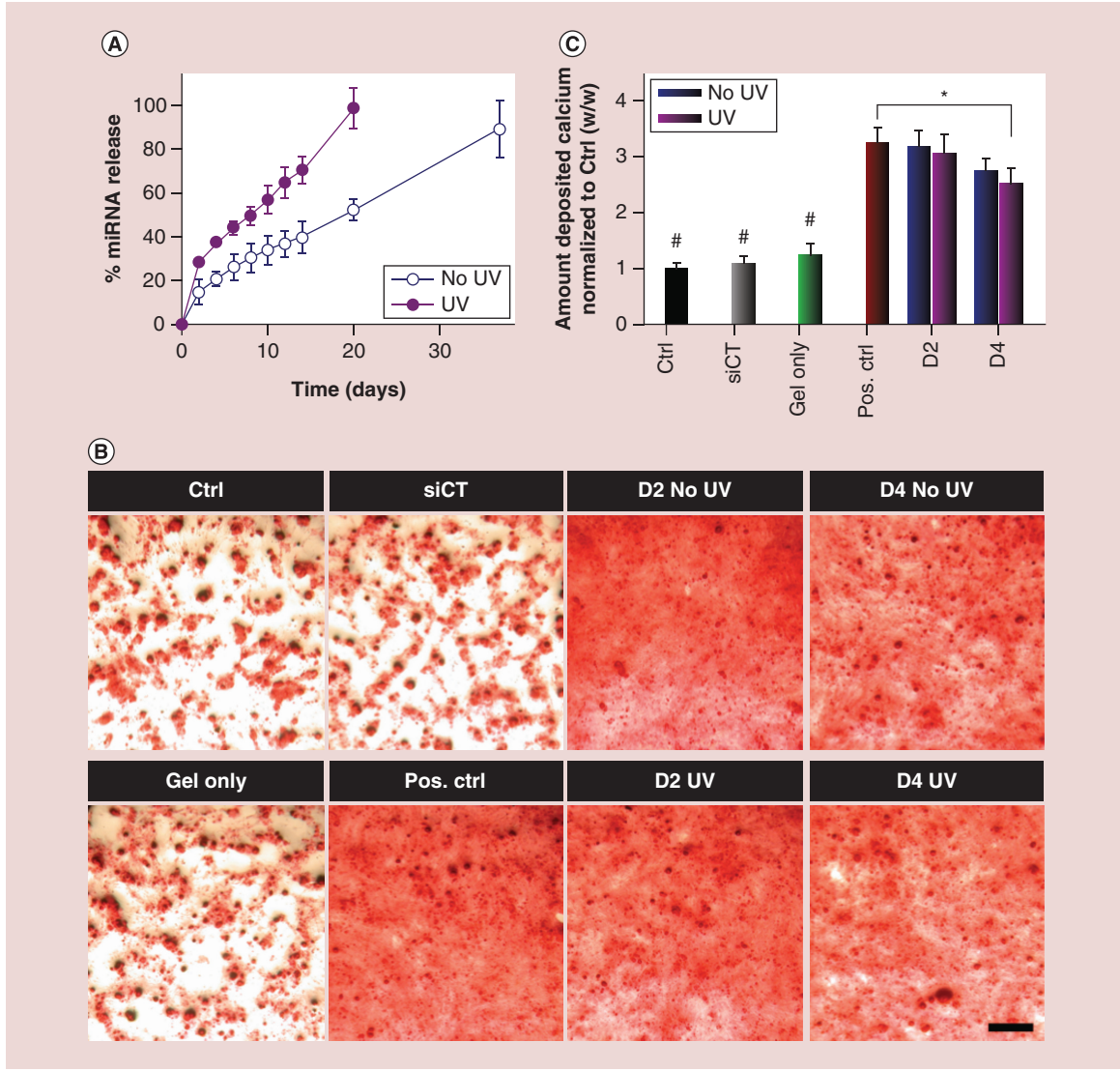

Figure 9. (A) miRNA-20a release behavior from 22.5% (w/v) photodegradable hydrogels into DMEM-LG in the absence or presence of 'UV 2–10' daily. **(B)** Photomicrographs of ARS staining depicting the deposition of calcium and **(C)** quantification of deposited calcium (normalized to 'Ctrl') by hMSCs cultured in monolayer and transfected with the same concentration (40 nM) of released miRNA-20a from hydrogels at day 2 (D2) or day 4 (D4) or freshly reconstituted lyophilized RNA/PEI complexes of siCT ('siCT') or miRNA-20a ('Pos. Ctrl'). 'Gel only': pooled D4 releasates from 'UV'-treated hydrogels lacking RNA. The scale bar indicates 200 μm.
#$p < 0.01$ compared with groups that do not contain the same symbol.
*$p < 0.05$.

Again, these results demonstrated that the UV light application to the hydrogels not only accelerated RNA release, but also permitted retention of its bioactivity.

Conclusion

A dual-crosslinked *in situ* forming photodegradable hydrogel was developed for actively controlling the release of either unmodified or chemically modified siRNA or miRNA via UV irradiation. Photodegradable linkages were introduced into the hydrogel network to control the degradation rate of the hydrogels and subsequently to trigger the release of the loaded genetic materials upon the application of UV light. UV-triggered, accelerated release of siGFP exhibited high bioactivity by silencing GFP expression of deGFP-expressing HeLa cells to the same degree as the freshly prepared siGFP. Importantly, the UV-triggered, accelerated release of siNoggin or miRNA-20a from the hydrogel system induced the osteogenic differentiation of hMSCs, demonstrating the potential for applying this photodegradable hydrogel system for bone regeneration. To the best of our knowledge, this is the first photodegradable hydrogel system that can provide the 'on-demand' delivery of unmodified RNAs at designated time points via the application of an external stimulus in the form of UV light. This hydrogel system provides an excellent platform for 'on-demand' release of genetic materials or other bioactive agents at a specific time via externally applied UV, and is promising for applications in disease therapeutics and tissue regeneration.

Supplementary data

To view the supplementary data that accompany this paper please visit the journal website at: www.futuremedicine.com/doi/full/10.2217/nnm-2016-0088

Financial & competing interests disclosure

The authors acknowledge funding from the National Institutes of Health (R01AR063194, R56DE022376 [E Alsberg] and GM077173 [V Rotello]) and the Department of Defense Congressionally Directed Medical Research Programs (OR110196 [E Alsberg]). The authors have no other relevant affiliations or financial involvement with any organization or entity with a financial interest in or financial conflict with the subject matter or materials discussed in the manuscript apart from those disclosed.

No writing assistance was utilized in the production of this manuscript.

Executive summary

- Photodegradable dual-crosslinked poly(ethylene glycol)-based hydrogels were fabricated using two synergistic chemistries: Michael-type acrylate-thiol and oxidized disulfide formations.
- Photocleavable moieties were introduced into the hydrogel network, providing an active means to increase the hydrogel degradation rate post-gelation, and subsequently accelerate the release rate of encapsulated RNA/PEI complexes at designated time points.
- Disulfide bonds that degrade slowly via hydrolysis were employed to prolong the hydrogel persistence time and consequently the RNA release time course.
- In the absence of UV light, the loaded unmodified RNA complexed with PEI was released from the hydrogels in a sustained and controlled fashion.
- Upon the application of UV light, the release of the complexes (i.e., siLuc, siGFP, siNoggin and miRNA-20a) from the photodegradable hydrogels was accelerated, which was not observed in non-photodegradable hydrogels.
- Regardless of the presence of UV light, released siGFP exhibited high bioactivity by silencing GFP expression in deGFP-expressing HeLa cells cultured in monolayer.
- Released siNoggin and miRNA-20a from the hydrogels induced osteogenic differentiation of human mesenchymal stem cells to a similar extent as freshly reconstituted RNA.
- UV light exposure did not affect the bioactivity of the released RNA material from this photodegradable hydrogel system.
- This is the first report of a photodegradable hydrogel system that can provide the 'on-demand' accelerated delivery of unmodified RNA complexed with PEI at designated time points via the application of UV light, an external and user-controlled stimulus
- This photolabile hydrogel system provides a potentially valuable physician or patient-controlled 'on demand' RNA delivery platform for biomedical applications.

References

Papers of special note have been highlighted as: • of interest; •• of considerable interest

1 Hill MC, Nguyen MK, Jeon O, Alsberg E. Spatial control of cell gene expression by siRNA gradients in biodegradable hydrogels. *Adv. Healthcare Mater.* 4(5), 714–722 (2015).

2 Hoffman AS. Hydrogels for biomedical applications. *Adv. Drug Deliv. Rev.* 64(Suppl.), 18–23 (2012).

3 Vacanti JP, Langer R. Tissue engineering: the design and fabrication of living replacement devices for surgical reconstruction and transplantation. *Lancet* 354(Suppl. 1), SI32–SI34 (1999).

4 Jakab K, Marga F, Norotte C, Forgacs G. 4. The promises of tissue engineering for organ building and banking. *Cryobiology* 71(1), 165–166 (2015).

5 Berthiaume F, Maguire TJ, Yarmush ML. Tissue engineering and regenerative medicine: history, progress, and challenges. *Annu. Rev. Chem. Biomol. Eng.* 2, 403–430 (2011).

6 Nguyen MK, Jeon O, Krebs MD, Schapira D, Alsberg E. Sustained localized presentation of RNA interfering molecules from *in situ* forming hydrogels to guide stem cell osteogenic differentiation. *Biomaterials* 35(24), 6278–6286 (2014).

• **The first report of macroscopic hydrogels used for localized and sustained presentation of RNA interfering molecules in *in situ* forming hydrogels to guide the osteogenic differentiation of encapsulated stem cells.**

7 Andersen MO, Nygaard JV, Burns JS *et al.* siRNA nanoparticle functionalization of nanostructured scaffolds enables controlled multilineage differentiation of stem cells. *Mol. Ther.* 18(11), 2018–2027 (2010).

8 Hemming S, Cakouros D, Isenmann S *et al.* EZH2 and KDM6A act as an epigenetic switch to regulate mesenchymal stem cell lineage specification. *Stem Cells* 32(3), 802–815 (2014).

9 Zhang JF, Fu WM, He ML *et al.* MiRNA-20a promotes osteogenic differentiation of human mesenchymal stem cells by co-regulating BMP signaling. *RNA Biol.* 8(5), 829–838 (2011).

10 Kondo M, Yamaoka K, Sakata K *et al.* Contribution of the interleukin-6/STAT-3 signaling pathway to chondrogenic differentiation of human mesenchymal stem cells. *Arthritis Rheum.* 67(5), 1250–1260 (2015).

11 Chen L, Holmstrøm K, Qiu W *et al.* MicroRNA-34a inhibits osteoblast differentiation and *in vivo* bone formation of human stromal stem cells. *Stem Cells* 32(4), 902–912 (2014).

12 Tzeng SY, Hung BP, Grayson WL, Green JJ. Cystamine-terminated poly(beta-amino ester)s for siRNA delivery to human mesenchymal stem cells and enhancement of osteogenic differentiation. *Biomaterials* 33(32), 8142–8151 (2012).

13 Pittenger MF, MacKay AM, Beck SC *et al.* Multilineage potential of adult human mesenchymal stem cells. *Science* 284(5411), 143–147 (1999).

14 Branch MJ, Hashmani K, Dhillon P, Jones DR, Dua HS, Hopkinson A. Mesenchymal stem cells in the human corneal limbal stroma. *Invest. Ophthalmol. Vis. Sci.* 53(9), 5109–5116 (2012).

15 Wang S, Qu X, Zhao RC. Clinical applications of mesenchymal stem cells. *J. Hematol. Oncol.* 5, 19 (2012).

16 Dang PN, Dwivedi N, Yu X *et al.* Guiding chondrogenesis and osteogenesis with mineral-coated hydroxyapatite and BMP-2 incorporated within high-density hMSC aggregates for bone regeneration. *ACS Biomater. Sci. Eng.* 2(1), 30–42 (2016).

17 Chu CY, Rana TM. Translation repression in human cells by microRNA-induced gene silencing requires RCK/p54. *PLoS Biol.* 4(7), e210 (2006).

18 Lam JKW, Chow MYT, Zhang Y, Leung SWS. siRNA versus miRNA as therapeutics for gene silencing. *Mol. Ther. Nucleic Acids* 4, e252 (2015).

19 Davis ME, Zuckerman JE, Choi CHJ *et al.* Evidence of RNAi in humans from systemically administered siRNA via targeted nanoparticles. *Nature* 464(7291), 1067–1070 (2010).

• **This is the first report of a clinical trial using systemically administered siRNA for liver cancer treatment.**

20 Tabernero J, Shapiro GI, Lorusso PM *et al.* First-in-humans trial of an RNA interference therapeutic targeting VEGF and KSP in cancer patients with liver involvement. *Cancer Discov.* 3(4), 406–417 (2013).

21 Segovia N, Pont M, Oliva N, Ramos V, Borros S, Artzi N. Hydrogel doped with nanoparticles for local sustained release of siRNA in breast cancer. *Adv. Healthcare Mater.* 4, 271–280 (2015).

22 Sengupta A, Mezencev R, Mcdonald JF, Prausnitz MR. Delivery of siRNA to ovarian cancer cells using laser-activated carbon nanoparticles. *Nanomedicine* 10(11), 1775–1784 (2015).

23 Kim Y-D, Park T-E, Singh B *et al.* Nanoparticle-mediated delivery of siRNA for effective lung cancer therapy. *Nanomedicine* 10(7), 1165–1188 (2015).

24 Nelson CE, Gupta MK, Adolph EJ, Guelcher SA, Duvall CL. siRNA delivery from an injectable scaffold for wound therapy. *Adv. Wound Care* 2(3), 93–99 (2012).

25 Yin L, Zhao X, Ji S *et al.* The use of gene activated matrix to mediate effective SMAD2 gene silencing against hypertrophic scar. *Biomaterials* 35(8), 2488–2498 (2014).

26 Charafeddine RA, Makdisi J, Schairer D *et al.* Fidgetin-Like 2: a microtubule-based regulator of wound healing. *J. Invest. Dermatol.* 135(9), 2309–2318 (2015).

27 Nelson CE, Kim AJ, Adolph EJ *et al.* Tunable delivery of siRNA from a biodegradable scaffold to promote angiogenesis *in vivo*. *Adv. Mater.* 26(4), 607–614 (2014).

• **An important report of biomaterial scaffold used for localized and sustained presentation of siRNA to promote the formation of vascular tissue.**

28 Ramasubramanian A, Shiigi S, Lee G, Yang F. Non-viral delivery of inductive and suppressive genes to adipose-derived stem cells for osteogenic differentiation. *Pharm. Res.* 28(6), 1328–1337 (2011).

29 Takayama K, Suzuki A, Manaka T *et al.* RNA interference for noggin enhances the biological activity of bone morphogenetic proteins *in vivo* and *in vitro*. *J. Bone Miner. Metab.* 27(4), 402–411 (2009).

30 Deng Y, Bi X, Zhou H *et al.* Repair of critical-sized bone defects with anti-miR-31-expressing bone marrow stromal stem cells and poly(glycerol sebacate) scaffolds. *Eur. Cell. Mater.* 27, 13–24; discussion 24–15 (2014).

31 Liu H, Peng H, Wu Y *et al.* The promotion of bone regeneration by nanofibrous hydroxyapatite/chitosan scaffolds by effects on integrin-BMP/Smad signaling pathway in BMSCs. *Biomaterials* 34(18), 4404–4417 (2013).

32 Beavers KR, Nelson CE, Duvall CL. MiRNA inhibition in tissue engineering and regenerative medicine. *Adv. Drug. Deliv. Rev.* 88, 123–137 (2015).

33 Agrawal N, Dasaradhi PVN, Mohmmed A, Malhotra P, Bhatnagar RK, Mukherjee SK. RNA interference: biology, mechanism, and applications. *Microbiol. Mol. Biol. Rev.* 67(4), 657–685 (2003).

34 Chen M, Gao S, Dong M *et al.* Chitosan/siRNA nanoparticles encapsulated in PLGA nanofibers for siRNA delivery. *ACS Nano* 6(6), 4835–4844 (2012).

35 Rettig GR, Behlke MA. Progress toward *in vivo* use of siRNAs-II. *Mol. Ther.* 20(3), 483–512 (2012).

36 Whitehead KA, Dahlman JE, Langer RS, Anderson DG. Silencing or stimulation? siRNA delivery and the immune system. *Annu. Rev. Chem. Biomol. Eng.* 2, 77–96 (2011).

37 Whitehead KA, Langer R, Anderson DG. Knocking down barriers: advances in siRNA delivery. *Nat. Rev. Drug Discov.* 8(2), 129–138 (2009).

38 Nguyen MK, Alsberg E. Bioactive factor delivery strategies from engineered polymer hydrogels for therapeutic medicine. *Prog. Polym. Sci.* 39(7), 1235–1265 (2014).

39 Krebs MD, Jeon O, Alsberg E. Localized and sustained delivery of silencing RNA from macroscopic biopolymer hydrogels. *J. Am. Chem. Soc.* 131(26), 9204–9206 (2009).

- **This is the first report of the use of macroscopic hydrogels for localized and sustained release of bioactive siRNA.**

40 Krebs MD, Alsberg E. Localized, targeted, and sustained siRNA delivery. *Chem. Eur. J.* 17(11), 3054–3062 (2011).

41 Nguyen K, Dang PN, Alsberg E. Functionalized, biodegradable hydrogels for control over sustained and localized siRNA delivery to incorporated and surrounding cells. *Acta Biomater.* 9(1), 4487–4495 (2013).

- **This is the first report of the use of macroscopic hydrogels for localized, sustained and controlled release of bioactive siRNA.**

42 Kim YM, Park MR, Song SC. An injectable cell penetrable nano-polyplex hydrogel for localized siRNA delivery. *Biomaterials* 34(18), 4493–4500 (2013).

43 Aagaard L, Rossi JJ. RNAi therapeutics: principles, prospects and challenges. *Adv. Drug Deliv. Rev.* 59(2–3), 75–86 (2007).

44 Bumcrot D, Manoharan M, Koteliansky V, Sah DWY. RNAi therapeutics: a potential new class of pharmaceutical drugs. *Nat. Chem. Biol.* 2(12), 711–719 (2006).

45 Gavrilov K, Saltzman WM. Therapeutic siRNA: principles, challenges, and strategies. *Yale J. Biol. Med.* 85(2), 187–200 (2012).

46 Hobel S, Aigner A, Polyethylenimines for siRNA and miRNAdelivery *in vivo. WIREsNanomed. Nanobiotechnol.* 5(5), 484–501 (2013).

- **This is an important report demonstrating the ability of polyethylenimines to delivery of siRNA and miRNA *in vivo*.**

47 Huynh CT, Nguyen MK, Tonga GY, Longé L, Rotello VM, Alsberg E. Photocleavable hydrogels for light-triggered siRNA release. *Adv. Healthcare Mater.* 5(3), 305–310 (2016).

- **This is the first report of UV light, an external and user-controlled stimulus, used to control the release of bioactive genetic material from macroscopic hydrogels.**

48 Zimmermann TS, Lee ACH, Akinc A *et al.* RNAi-mediated gene silencing in non-human primates. *Nature* 441(7089), 111–114 (2006).

49 Ghosn B, Singh A, Li M *et al.* Efficient gene silencing in lungs and liver using imidazole-modified chitosan as a nanocarrier for small interfering RNA. *Oligonucleotides* 20(3), 163–172 (2010).

50 Foster AA, Greco CT, Green MD, Epps TH III, Sullivan MO. Light-mediated activation of siRNA release in diblock copolymer assemblies for controlled gene silencing. *Adv. Healthcare Mater.* 4(5), 760–770 (2015).

51 Taratula O, Garbuzenko OB, Kirkpatrick P *et al.* Surface-engineered targeted PPI dendrimer for efficient intracellular and intratumoral siRNA delivery. *J. Control. Release* 140(3), 284–293 (2009).

52 Tamura A, Nagasaki Y. Smart siRNA delivery systems based on polymeric nanoassemblies and nanoparticles. *Nanomedicine* 5(7), 1089–1102 (2010).

53 Fischer NO, Rasley A, Blanchette C. Nanoparticles and antigen delivery: understanding the benefits and drawbacks of different delivery platforms. *Nanomedicine* 9(4), 373–376 (2014).

54 Xue HY, Liu S, Wong HL. Nanotoxicity: a key obstacle to clinical translation of siRNA-based nanomedicine. *Nanomedicine* 9(2), 295–312 (2014).

55 Huynh CT, Nguyen MK, Lee DS. Injectable block copolymer hydrogels: achievements and future challenges for biomedical applications. *Macromolecules* 44(17), 6629–6636 (2011).

56 Van Vlierberghe S, Dubruel P, Schacht E. Biopolymer-based hydrogels as scaffolds for tissue engineering applications: a review. *Biomacromolecules* 12(5), 1387–1408 (2011).

57 Nguyen QV, Huynh DP, Park JH, Lee DS. Injectable polymeric hydrogels for the delivery of therapeutic agents: a review. *Eur. Polym. J.* 72, 602–619 (2015).

58 Ren K, He C, Xiao C, Li G, Chen X. Injectable glycopolypeptide hydrogels as biomimetic scaffolds for cartilage tissue engineering. *Biomaterials* 51, 238–249 (2015).

59 Huynh CT, Nguyen MK, Jeong IK, Kim SW, Lee DS. Synthesis, characteristics and potential application of poly (β-amino ester urethane)-based multiblock co-polymers as an injectable, biodegradable and pH/temperature-sensitive hydrogel system. *J. Biomat. Sci. Polym. Edn* 23(8), 1091–1106 (2012).

60 Loh XJ, Guerin W, Guillaume SM. Sustained delivery of doxorubicin from thermogelling poly (PEG/PPG/PTMC urethane) s for effective eradication of cancer cells. *J. Mater. Chem.* 22(39), 21249–21256 (2012).

61 Cheng Y, He C, Ding J, Xiao C, Zhuang X, Chen X. Thermosensitive hydrogels based on polypeptides for localized and sustained delivery of anticancer drugs. *Biomaterials* 34(38), 10338–10347 (2013).

62 Tokatlian T, Cam C, Segura T. Non-viral DNA delivery from porous hyaluronic acid hydrogels in mice. *Biomaterials* 35(2), 825–835 (2014).

63 Huynh CT, Nguyen QV, Kang SW, Lee DS. Synthesis and characterization of poly(amino urea urethane)-based block copolymer and its potential application as injectable pH/temperature-sensitive hydrogel for protein carrier. *Polymer* 53(19), 4069–4075 (2012).

64 Nguyen MK, Huynh CT, Gao GH *et al.* Biodegradable oligo (amidoamine/β-amino ester) hydrogels for controlled insulin delivery. *Soft Matter* 7(6), 2994–3001 (2011).

65 Huynh CT, Nguyen MK, Lee DS. Dually cationic and anionic pH/temperature-sensitive injectable hydrogels and potential application as a protein carrier. *Chem. Commun.* 48(89), 10951–10953 (2012).

66 Stanford CM, Jacobson PA, Eanes ED, Lembke LA, Midura RJ. Rapidly forming apatitic mineral in an osteoblastic cell line (UMR 10601 BSP). *J. Biol. Chem.* 270(16), 9420–9428 (1995).

67 Larsen SA, Kassem M, Rattan SI. Glucose metabolite glyoxal induces senescence in telomerase-immortalized human mesenchymal stem cells. *Chem. Cent. J.* 6(1), 18 (2012).

68 Gregory CA, Gunn WG, Peister A, Prockop DJ. An Alizarin red-based assay of mineralization by adherent cells in culture: comparison with cetylpyridinium chloride extraction. *Anal. Biochem.* 329(1), 77–84 (2004).

69 Kloxin AM, Kasko AM, Salinas CN, Anseth KS. Photodegradable hydrogels for dynamic tuning of physical and chemical properties. *Science* 324(5923), 59–63 (2009).

•• **This is the first report of photolabile moieties in a hydrogel network used for dynamic tuning of hydrogel physical and chemical properties using externally applied UV light.**

70 Griffin DR, Kasko AM. Photodegradable macromers and hydrogels for live cell encapsulation and release. *J. Am. Chem. Soc.* 134(31), 13103–13107 (2012).

71 Vermonden T, Censi R, Hennink WE. Hydrogels for protein delivery. *Chem. Rev.* 112(5), 2853–2888 (2012).

72 Heliotis M, Tsiridis E. Suppression of bone morphogenetic protein inhibitors promotes osteogenic differentiation: therapeutic implications. *Arthritis Res. Ther.* 10(4), 115–115 (2008).

73 Bassit ACF, Moffatt P, Gaumond M-H, Hamdy R. The potential use of nanoparticles for noggin siRNA delivery to accelerate bone formation in distraction osteogenesis. *J. Nanomed. Nanotech.* 6(1), 257 (2015).

74 Kwong FN, Richardson SM, Evans CH. Chordin knockdown enhances the osteogenic differentiation of human mesenchymal stem cells. *Arthritis Res. Ther.* 10(3), R65 (2008).

75 Lavery K, Swain P, Falb D, Alaoui-Ismaili MH. BMP-2/4 and BMP-6/7 differentially utilize cell surface receptors to induce osteoblastic differentiation of human bone marrow-derived mesenchymal stem cells. *J. Biol. Chem.* 283(30), 20948–20958 (2008).

76 Lin T-H, Yang R-S, Tang C-H, Lin C-P, Fu W-M. PPARγ inhibits osteogenesis via the down-regulation of the expression of COX-2 and iNOS in rats. *Bone* 41(4), 562–574 (2007).

77 Bosio V, Dubreuil F, Bogdanovic G, Fery A. Interactions between silica surfaces coated by polyelectrolyte multilayers in aqueous environment: comparison between precursor and multilayer regime. *Colloids Surf. A Physicochem. Eng. Asp.* 243(1–3), 147–155 (2004).

78 Meneksedag-Erol D, Tang T, Uludag H. Probing the effect of miRNA on siRNA-PEI polyplexes. *J. Phys. Chem. B* 119(17), 5475–5486 (2015).

79 Gratton SEA, Ropp PA, Pohlhaus PD *et al.* The effect of particle design on cellular internalization pathways. *Proc. Natl Acad. Sci. USA* 105(33), 11613–11618 (2008).